Letter

Anomalous anisotropy of the lower critical field and Meissner effect in UTe_2

C. Paulsen,[1,*] G. Knebel,[2] G. Lapertot,[2] D. Braithwaite,[2] A. Pourret,[2] D. Aoki,[2,3] F. Hardy,[4] J. Flouquet,[2] and J.-P. Brison[2]

[1]*Université Grenoble Alpes, Institut Néel, CNRS BP 166, F-38042 Grenoble France*

[2]*Université Grenoble Alpes, CEA, Grenoble INP, IRIG, PHELIQS, F-38000 Grenoble, France*

[3]*Institute for Materials Research, Tohoku University, Ibaraki 311-1313, Japan*

[4]*Institute for Solid-State Physics, Karlsruhe Institute of Technology, D-76021 Karlsruhe, Germany*

(Received 28 February 2020; revised 10 April 2021; accepted 13 April 2021; published 5 May 2021)

We report on low-temperature susceptibility and magnetization measurements made on single crystals of the recently discovered heavy-fermion superconductor UTe_2 and compare the results with the two ambient pressure ferromagnetic superconductors URhGe and UCoGe. Hysteresis curves in the superconducting phase show a familiar diamond shape superimposed on a large paramagnetic background. The Meissner state was measured by zero-field cooling in small fields of a few Oe as well as ac susceptibility measurements in small fields and resulted in 100% shielding, with a sharp transition. However, the field-cooling Meissner-Ochsenfeld effect (expulsion of flux) was negligible in fields greater than just a few Oe, but becomes nearly 30% of the perfect diamagnetic signal when the field was reduced to 0.01 Oe. The critical current due to flux pinning was studied by ac susceptibility techniques. Over the range in fields and temperature of this study, no signature of a ferromagnetic transition could be discerned. The lower critical field H_{c1} has been measured along the three crystallographic axes, and surprisingly, the anisotropy of H_{c1} contradicts that of the upper critical field. We discuss this discrepancy and show that it may provide additional support for a magnetic field-dependent pairing mediated by ferromagnetic fluctuations in UTe_2.

DOI: 10.1103/PhysRevB.103.L180501

Spin-triplet superconductivity (SC) in itinerant ferromagnets close to the ferromagnetic (FM)-paramagnetic (PM) instability was proposed four decades ago [1]. The discovery of the coexistence of ferromagnetism and SC in UGe_2 opened the "rush" to a large variety of experiments [2]. The strong first-order nature of the FM-PM transition under pressure at $p_c \approx 1.6$ GPa leads to SC occurring only in the FM domain in the pressure range from 1.2 to 1.6 GPa; the maximum of the superconducting temperature T_c is 0.8 K, but the Curie temperature $T_{Curie} \approx 30$ K [3].

The field was enriched by the discoveries of two ambient pressure superconducting ferromagnets, URhGe [4] and UCoGe [5], with $T_c = 0.25$ and 0.8 K, much lower than the respective $T_{Curie} = 9.5$ and 2.7 K. The rapid suppression of T_{Curie} in UCoGe with pressure leads a the PM ground state above 1 GPa with the persistence of SC far above the critical pressure [6]. For both systems, the weakness of the FM interaction means that transverse magnetic fields (H) applied along the b axis, perpendicular to the easy magnetization axis c, of these orthorhombic crystals give rise to a spectacular field enhancement of SC [3,7,8].

The recent observation of SC in orthorhombic UTe_2 [9,10] at $T_c = 1.6$ K opens the possibility to study at ambient pressure spin-triplet SC in a system with a PM ground state located very close to a PM-FM instability. UTe_2 has the highest susceptibility [11] and strong magnetic fluctuations [12] along the a axis. However, the transverse field configuration with $H \parallel b$ attracted the most attention, due to the observation of a strong field-induced reinforcement of SC on approaching the metamagnetic field $H_m \approx 35$ T [13–16]. Most of the published magnetization data in FM SC investigate the field dependence of the FM interaction by longitudinal or transverse field variation [17–19].

In URhGe and UCoGe the respective FM sublattice magnetization $M_0 = 0.4\mu_B$ and $0.07\mu_B$ per U atom produces an internal field of 800 and 100 G far higher than the estimated value of the lower superconducting critical field H_{c1} of a few gauss. Thus even at $H = 0$, self-induced vortices should occur, as shown for example in the magnetization studies on UCoGe [20].

In this Letter we report low-temperature susceptibility and magnetization measurements on two crystals of UTe_2 ($T_c = 1.5$ and 1.6 K). The experiments concentrate on (i) the persistence of the PM state well below T_c K, (ii) the strength of the Meissner effect in field-cooled (FC) experiments, (iii) the proof of a complete superconducting screening in zero-field-cooled (ZFC) magnetization measurements, (iv) the determination of H_{c1}, and (v) the determination of the London penetration depth and of the superconducting coherence length from H_{c1} and from the upper critical field H_{c2}. We compare the results with the FM superconductors URhGe and UCoGe [21].

All the measurements were made using two low-temperature superconducting quantum interference device (SQUID) magnetometers developed at the Institut Néel in Grenoble. A unique feature of the setup is that absolute values of the magnetization can be measured using the extraction method in a field range from 0.01 Oe up to 8 T (for details, see the Supplemental Material [21]).

*carley.paulsen@neel.cnrs.fr

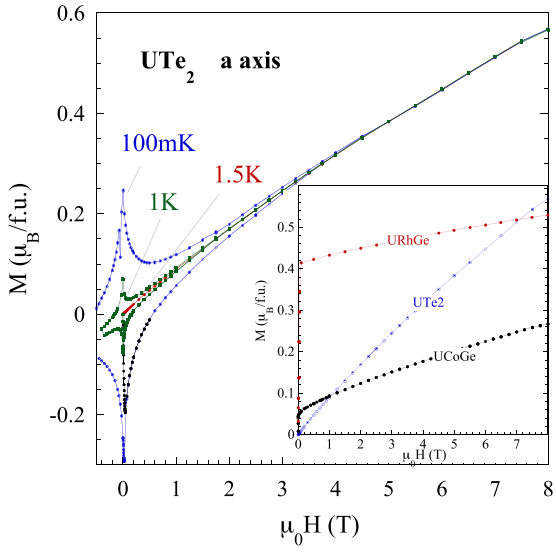

FIG. 1. Magnetization vs field for UTe_2 (sample 1) at 100 mK and 1 K below T_c, and at 1.5 K just above T_c in the normal state with the field along the *a* axis (easy axis). The inset shows the magnetization of UTe_2 (blue) at 1.5 K, URhGe (red) at 500 mK, and UCoGe (black) at 600 mK, i.e., just above their respective T_c in the normal state, with the field along the easy axis.

Figure 1 shows hysteresis loops for UTe_2 measured at 100 mK and 1 K below T_c, and at 1.5 K in the normal phase for UTe_2 with the field direction along the easy magnetization *a* axis. The slope of the initial magnetization [also shown later more clearly in Fig. 4(a)] corresponds to 100% shielding. The inset of Fig. 1 compares UTe_2 at 1.5 K to the two FM superconductors URhGe and UCoGe, with the field applied along their easy *c* axis, at 500 and 600 mK above their respective superconducting states, but far below their respective Curie temperatures. The spontaneous moment of both ferromagnetic superconductors appears clearly, however, it is not a saturated moment: $M(H)$ keeps growing with increasing field. Although there is no spontaneous moment for UTe_2, the PM magnetization increases quickly and becomes larger than in UCoGe at about 1 T, and then greater than in URhGe above 7 T.

The hysteresis loops for UTe_2 have a familiar superconducting diamond shape which is superimposed on a very large PM background response. More hysteresis loops taken close to T_c are shown in Fig. S5 in the Supplemental Material, as well as a comparison with UCoGe in Figs. S6 and S7. In contrast to UCoGe where the superconducting and FM signals are fused together with the FM response dominating [20], our measurements of UTe_2 over the full temperature and field range show that there is no hint of FM behavior down to 80 mK, in agreement with muon spin rotation (4μSR) experiments [22].

In Fig. 2(a) the dc susceptibility M/H is plotted against temperature for various applied fields ranging from 0.01 to 200 Oe. Each curve was made by first zero-field cooling (ZFC) the sample. A dc field was then applied and the sample was slowly warmed above T_c, after which it was recooled in the same field, giving the field-cooled (FC) curve. In small dc fields the value of the ZFC susceptibility corresponds to

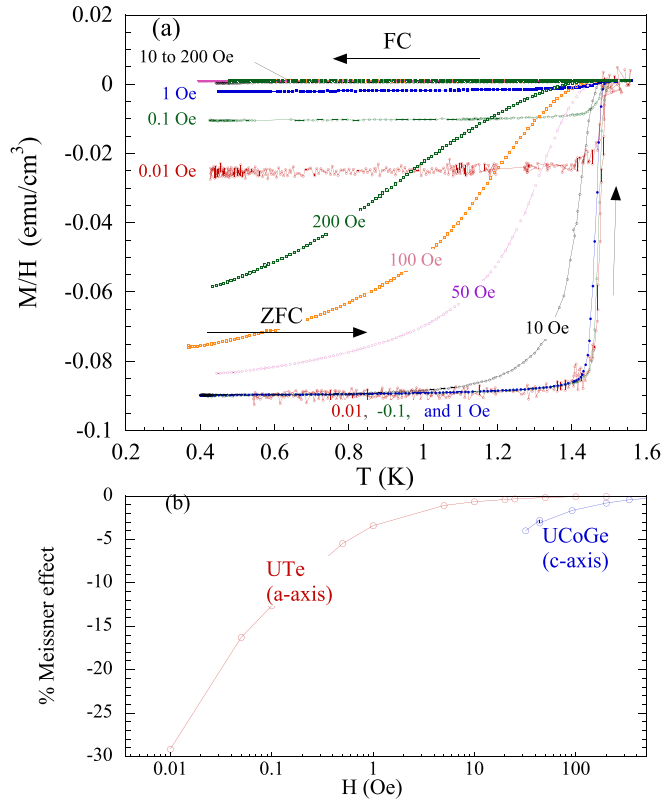

FIG. 2. (a) M/H vs T of UTe_2 (sample 1) for various applied fields ranging from 0.01 to 200 Oe from zero-field-cooled (ZFC) and field-cooled (FC) measurements. (b) The percent Meissner-Ochsenfeld effect (expulsion of flux) plotted against the applied field for UTe_2 (red points) and for UCoGe (blue points). Note that the field range in UCoGe cannot extend below 100 mT as the sample needs to be monodomain. Over the comparable field range, the expulsion of flux is much greater in UCoGe.

100% shielding of the field (when demagnetization corrections are made), and the transition is sharp. As the fields are increased, the transition becomes broader and shifts to lower temperatures. The FC susceptibility shows that the Meissner-Ochsenfeld effect (the reversible expulsion of flux as the sample is field-cooled and warmed through T_c) for fields greater than a few Oe is negligible. However, for very small fields, the effect becomes more important, reaching about 30% expulsion in a field of 0.01 0e.

We compare this last result to UCoGe along the easy axis in Fig. 2(b). There are important differences. First, the internal fields that are present in UCoGe, of the order 50–100 G, are much greater than H_{c1}, and as a result UCoGe is always in the mixed state, and never achieves 100% shielding. In addition, to measure the Meissner-Ochsenfeld effect in UCoGe means taking into account hysteresis and a coercive field such that the applied field has no meaning while the sample is multidomain [20]. Nevertheless, a typical value of the percent expulsion of the flux from UCoGe compared to its effective shielding would be about 3% expulsion at 50 Oe, which decreases with increasing field. Although small, this is much greater than the Meissner-Ochsenfeld effect observed in UTe_2 in the same field range as can be seen in Fig. 2(b). The other remarkable feature observed in Fig. 2(b) is the nonsaturating rate of

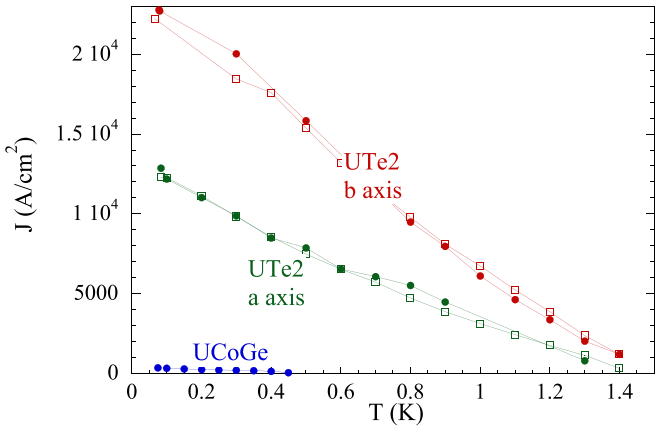

FIG. 3. Current density J_c derived from the critical state model vs temperature for UTe_2 (sample 2) measured along the a and b axes, and for UCoGe along the c axis. The solid round points are data derived from the imaginary part of ac susceptibility, and the open square points are data derived from the remanent magnetization (discussed in the Supplemental Material [21]).

increase of the Meissner effect down to fields as low as 0.01 Oe in UTe_2: If any internal field exists due to a weak FM phase inside the superconducting phase, the resulting dipolar field has to be much smaller than 0.01 G, or in other words, the ordered moment should be much smaller than $7 \times 10^{-6}\mu_B$.

A strong hysteresis and a weak Meissner-Ochsenfeld effect suggests strong flux pinning. To confirm this we measured the ac susceptibility χ as a function of the ac driving field: An example can be seen in the Supplemental Material Fig. S20 for the b axis. When flux begins to enter the sample, χ' and χ'' of the ac susceptibility will deviate from their 100% shielding values. The deviations are linear in the applied driving field and the slopes are proportional to $2/(J_cD)$ for χ', and $2/(3\pi J_cD)$ for χ'', where J_c is the current density in the critical state model, and D is the sample width, where we approximate the sample shapes as slabs [23]. The resulting $J_c(H)$ for UTe_2 is plotted in Fig. 3, along with J_c for UCoGe measured along the c axis. Clearly, flux pinning is far greater in UTe_2.

The initial magnetization M vs H taken at various constant temperatures is shown in Fig. 4(a). For each curve, the sample was first ZFC. The blue dashed line is a linear fit to the 100 mK data over a field range 0–10 Oe The slope of this fit (when corrected for demagnetization effects) corresponds to a susceptibility of $-1/4\pi$ (-1 in SI units) or 100% shielding of the magnetic field. For a given temperature, as the field is increased, the curves deviate from this slope, and this is an indication that flux is entering the sample because H_{c1} has been exceeded. As can be seen in Fig. 4(a), due to the strong pinning, flux enters the sample almost asymptotically and makes the determination of H_{c1} difficult. In addition, because the samples used in this study are not perfect ellipsoids, the field enters the samples sooner around the edges due to demagnetization effects, further obscuring the real H_{c1}.

A better way to determine H_{c1} is to measure the remanent magnetization as shown in Figs. 4(b) and 4(c) and discussed in detail in the Supplemental Material. Figure 4(b) is an example of a series of minor hysteresis loops at 1.1 K for sample 1

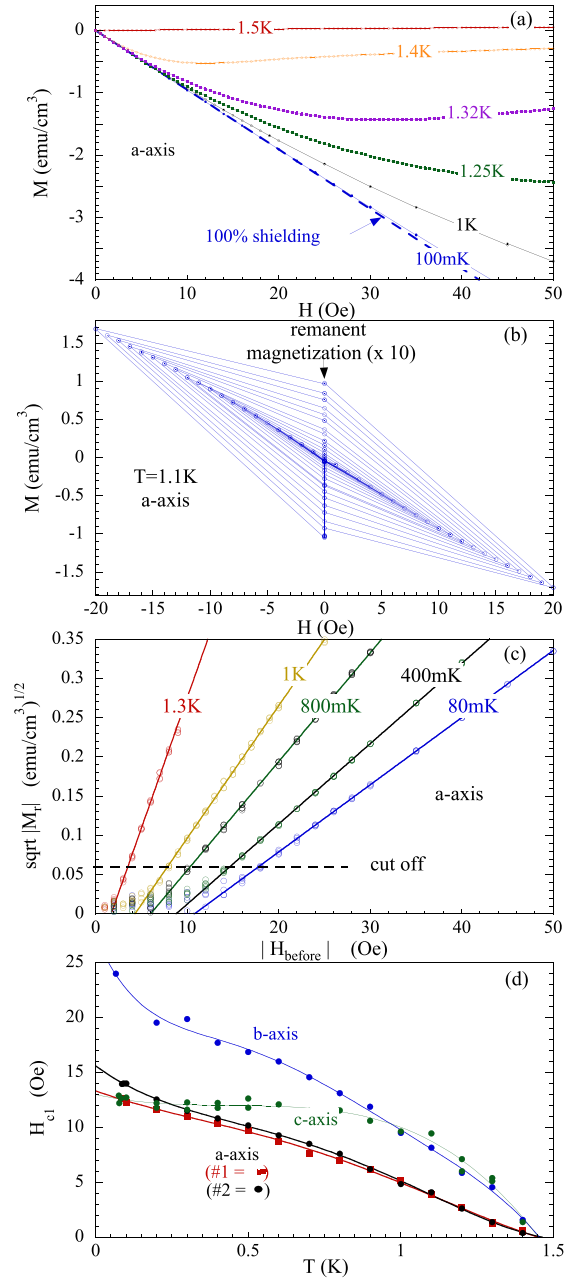

FIG. 4. (a) Initial magnetization M vs H taken a various constant temperatures for UTe_2 (sample 1) with the field along the a axis. The dashed line is a linear fit to the 100 mK data at low fields, and represents 100% shielding. (b) Series of minor hysteresis loops for sample 1 at 1.1 K where the magnitude of the field was systematically increased in steps of 1 Oe, and then returned to zero to measure the point at which a remanent magnetization begins to appear in the sample (the remanent magnetization has been multiplied by 10). (c) The remanent magnetization is plotted as $\sqrt{M_r}$ vs H_{before} for the a axis for sample 1. The solid lines are linear fits to the data above the cutoff line. (d) $H_{c1}(T)$ for UTe_2 along the a axis for sample 1 (red) and for sample 2 along the a (black), b (blue), and c (green) axis after correcting for demagnetization effects. The lines are guides to the eye.

where the magnitude of the field was systematically increased in small steps, and then returned to zero to measure the point where flux begins to enter the sample. While $H < H_{c1}(T)$

the cycles are reversible. However, when $H_{c1}(T)$ is exceeded, flux begins to enter the sample and the magnetization deviates from the 100% shielding. When the field is then returned to zero, half the flux remains trapped in the sample, and a remanent moment M_r appears. According to the Bean critical state model $M_r \propto H^2_{before}$, i.e., the last field value before the field was reduced to zero and the remanence was measured [24]. In order to estimate H_{c1}, we modify the critical state model following [25] by assuming two regimes: when $H_{before} < H_{c1}$, $M_r = 0$ and when $H_{before} > H_{c1}$, $M_r \propto (H_{before} - H_{c1})^2$.

In Fig. 4(c) we plot an example of the remanent magnetizations for sample 1 as $\sqrt{M_r}$ vs H_{before}. The solid lines are linear fits to the high-field data above the cutoff line, thus omitting the low-field values where we expect rounding to occur. The intercept gives H_{c1}.

In Fig. 4(d) H_{c1} along the a axis is plotted versus temperature for sample 1, and for sample 2 for the a, b, and c axes, where H_{c1} has been corrected for demagnetization effects: Both samples have a platelet shape, with the field applied parallel to the platelet, except for the c-axis measurements which was performed perpendicular to the surface. We estimate the value of H_{c1} at $T = 0$ to be 14 Oe along the a and c axis, and 24 Oe along the b axis.

We have also studied H_{c2} along the a axis using bulk ac susceptibility as shown in Fig. S21 of the Supplemental Material and we found $H_{c2}(0) = 5.4$ T along the a axis, in good agreement with published resistivity measurements [9,10].

However, a comparison of H_{c1} and H_{c2} data reveals a major inconsistency. Indeed, close to T_c in the Ginzburg-Landau (GL) regime, the anisotropy of H_{c1} should be opposite to that of H_{c2} as $H_{c1}H_{c2} = H_c^2(\ln\kappa + 0.49)$, where H_c is the (isotropic) thermodynamic critical field and $\kappa = \frac{\lambda}{\sqrt{2}\xi}$ the anisotropic GL parameter. Hence, neglecting the anisotropy of κ due to the logarithm, with $H^b_{c2} > H^a_{c2} \approx H^c_{c2}$, one expects $H^b_{c1} < H^a_{c1} \approx H^c_{c1}$. In contrast, Fig. 4(c) shows that the relative anisotropies anticipated from H_{c2} are wrong in all directions. Quantitatively, this is a major effect, as the measured H_{c1} anisotropy between a and (b, c) is a factor 3, whereas the H_{c2} anisotropy between (a, c) and b is between 3 and 5, depending on the measurements notably for $H \parallel b$ (see, e.g., Ref. [10]) [15,16].

Such a large discrepancy calls for an explanation. Measurement errors of H_{c1} for $H \parallel b$ might come from stronger pinning in this direction. The critical current has been found indeed twice as large for $H \parallel a$ [see Fig. 3(b)], but it is very unlikely that it could explain a factor of 10 error between the two directions. The sample geometries are also similar in both cases, excluding an explanation through a bad estimation of the demagnetization corrections.

So the next step is to question the estimate of H_{c1} from the relations with the GL parameter: For single-band s-wave superconductors, these relations hold even in very anisotropic cases (see, e.g., Ref. [26]). However, UTe_2 is most likely p-wave, multigap (as most other heavy-fermion superconductors), and topological [27]. The last feature, implying the existence of low-energy surface states might influence pinning, but if it has any influence on the determination of H_{c1}, it should also be reflected in the critical current measurements. More interestingly, the multigap character [or the nodal gap structure [28] for one-dimensional (1D) irreducible representations] has been shown, theoretically (e.g., Ref. [29]) and experimentally (e.g., Ref. [30]) to induce strong deviations of the anisotropy of the critical fields from the estimations through the GL parameter: But this holds at low temperature, not close to T_c.

Last, several works have reported double transitions in their UTe_2 crystals at zero pressure [31,32]. Note, however, that H_{c1} and H_{c2} measurements are only sensitive to the upper transition, until both transitions eventually cross under field, which does not happen below 8 T according to Ref. [32]. Hence, whatever the origin of this double transition (intrinsic or due to inhomogeneities), it cannot help to understand the reported anomalous relative anisotropies of H_{c1} and H_{c2}.

A possible explanation for the puzzling anisotropy of H_{c1}, which cannot be completely ruled out, is a low-field change of slope of H_{c2}. This is suggested for example by specific heat measurements [33], which find a weak anisotropy between a and b axis due to a strong curvature of H_{c2} along a (hence a much larger slope at low fields), but still a smaller slope along the c axis. This may partially help to reduce the discrepancy between a and b anisotropies of H_{c1} and H_{c2}, but is still not enough to explain the H_{c1} result, requiring $H^a_{c2} \gg H^b_{c2} \sim H^c_{c2}$.

A key to understanding this anomalous anisotropy might be to take into account that the pairing mechanism in UTe_2 can be tuned by a magnetic field [9,15], a mechanism inducing a change of slopes of H_{c2} [18,19], which is not taken into account by GL. A field-dependent pairing induces a field dependence of the "bare" critical temperature $T_c(H)$ that is independent of the mixed state formation, as well as of the Fermi velocities (v_F) [19]. Hence, with field-dependent pairing, both critical fields are functions of field (through T_c and v_F) and temperature and it is easy to show that the measured slope at T_{sc} is $\frac{dH_{ci}}{dT} = \frac{(\frac{\partial H_{ci}}{\partial T})_H}{1+\frac{dT_{sc}}{dH}(\frac{\partial H_{ci}}{\partial T})_H}$. Here, $(\frac{\partial H_{ci}}{\partial T})_H$ is the "usual" slope defined for field-independent pairing, for which GL relations should hold. This relation between the measured $\frac{dH_{ci}}{dT}$ and $\frac{\partial H_{ci}}{\partial T}$ shows that, because H_{c1} is three to four orders of magnitudes smaller than H_{c2}, corrections due to $\frac{dT_{sc}}{dH}$ should be negligible on H_{c1}, which should reflect the true bare anisotropies. A $\frac{dT_{sc}}{dH} \approx -0.1$ T/K for $H \parallel a$ and $+0.1$ T/K for $H \parallel b$, (assuming $\frac{dT_{sc}}{dH} \approx 0$ for $H \parallel c$) could reconcile the lower and upper critical field measurements (see Supplemental Material for more details [21]).

To summarize, the surprising contradiction between lower and upper critical field anisotropies can be understood as a manifestation of the strong field dependence of the pairing strength in UTe_2, which is strongly suppressed along the easy axis and boosted along the hard b axis. Moreover, this is an indication that pairing is suppressed by a field along the easy axis in this system, an effect comparable to, although weaker than, in UCoGe [18,19], which can be seen as additional support for ferromagnetic fluctuation mediated pairing.

Moreover, from our very low-field measurements of the Meissner state, we can put an upper limit to any FM ordered moment above 100 mK of $7 \times 10^{-6}\mu_B$ in UTe_2. Restricted Meissner-Ochsenfeld expulsion is coherent with the observed strong pinning. A possible link between the present strong

pinning and singular topological properties of the superconducting phase deserve to be clarified.

We thank K. Behnia and T. Klein for fruitful discussions. We acknowledge the financial support of the Cross-Disciplinary Program on Instrumentation and Detection of CEA, the French Alternative Energies and Atomic Energy Commission, and KAKENHI (Grants No. JP15H05882, No. JP15H05884, No. JP15K21732, No. JP16H04006, No. JP15H05745, and No. JP19H00646).

[1] D. Fay and J. Appel, Phys. Rev. B **22**, 3173 (1980).
[2] S. S. Saxena, P. Agarwal, K. Ahilan, F. M. Grosche, R. K. W. Haselwimmer, M. J. Steiner, E. Pugh, I. R. Walker, S. R. Julian, P. Monthoux, G. G. Lonzarich, A. Huxley, I. Sheikin, D. Braithwaite, and J. Flouquet, Nature (London) **406**, 587 (2000).
[3] D. Aoki, K. Ishida, and J. Flouquet, J. Phys. Soc. Jpn. **88**, 022001 (2019).
[4] D. Aoki, A. D. Huxley, E. Ressouche, D. Braithwaite, J. Flouquet, J. Brison, E. Lhotel, and C. Paulsen, Nature (London) **413**, 613 (2001).
[5] N. T. Huy, A. Gasparini, D. E. de Nijs, Y. Huang, J. C. P. Klaasse, T. Gortenmulder, A. de Visser, A. Hamann, T. Görlach, and H. v. Löhneysen, Phys. Rev. Lett. **99**, 067006 (2007).
[6] G. Bastien, D. Braithwaite, D. Aoki, G. Knebel, and J. Flouquet, Phys. Rev. B **94**, 125110 (2016).
[7] F. Lévy, I. Sheikin, B. Grenier, and A. D. Huxley, Science **309**, 1343 (2005).
[8] D. Aoki, T. D. Matsuda, V. Taufour, E. Hassinger, G. Knebel, and J. Flouquet, J. Phys. Soc. Jpn. **78**, 113709 (2009).
[9] S. Ran, C. Eckberg, Q.-P. Ding, Y. Furukawa, T. Metz, S. R. Saha, I.-L. Liu, M. Zic, H. Kim, J. Paglione, and N. P. Butch, Science **365**, 684 (2019).
[10] D. Aoki, A. Nakamura, F. Honda, D. Li, Y. Homma, Y. Shimizu, Y. J. Sato, G. Knebel, J.-P. Brison, A. Pourret, D. Braithwaite, G. Lapertot, Q. Niu, M. Vališka, H. Harima, and J. Flouquet, J. Phys. Soc. Jpn. **88**, 043702 (2019).
[11] S. Ikeda, H. Sakai, D. Aoki, Y. Homma, E. Yamamoto, A. Nakamura, Y. Shiokawa, Y. Haga, and Y. Ōnuki, J. Phys. Soc. Jpn. **75**, 116 (2006).
[12] Y. Tokunaga, H. Sakai, S. Kambe, T. Hattori, N. Higa, G. Nakamine, S. Kitagawa, K. Ishida, A. Nakamura, Y. Shimizu, Y. Homma, D. Li, F. Honda, and D. Aoki, J. Phys. Soc. Jpn. **88**, 073701 (2019).
[13] A. Miyake, Y. Shimizu, Y. J. Sato, D. Li, A. Nakamura, Y. Homma, F. Honda, J. Flouquet, M. Tokunaga, and D. Aoki, J. Phys. Soc. Jpn. **88**, 063706 (2019).
[14] W. Knafo, M. Valika, D. Braithwaite, G. Lapertot, G. Knebel, A. Pourret, J.-P. Brison, J. Flouquet, and D. Aoki, J. Phys. Soc. Jpn. **88**, 063705 (2019).
[15] G. Knebel, W. Knafo, A. Pourret, Q. Niu, M. Valika, D. Braithwaite, G. Lapertot, M. Nardone, A. Zitouni, S. Mishra, I. Sheikin, G. Seyfarth, J.-P. Brison, D. Aoki, and J. Flouquet, J. Phys. Soc. Jpn. **88**, 063707 (2019).
[16] S. Ran, I.-L. Liu, Y. S. Eo, D. J. Campbell, P. M. Neves, W. T. Fuhrman, S. R. Saha, C. Eckberg, H. Kim, D. Graf, F. Balakirev, J. Singleton, J. Paglione, and N. P. Butch, Nat. Phys. **15**, 1250 (2019).
[17] F. Hardy, D. Aoki, C. Meingast, P. Schweiss, P. Burger, H. V. Löhneysen, and J. Flouquet, Phys. Rev. B **83**, 195107 (2011).
[18] S. Nakamura, T. Sakakibara, Y. Shimizu, S. Kittaka, Y. Kono, Y. Haga, J. Pospíšil, and E. Yamamoto, Phys. Rev. B **96**, 094411 (2017).
[19] B. Wu, G. Bastien, M. Taupin, C. Paulsen, L. Howald, D. Aoki, and J.-P. Brison, Nat. Commun. **8**, 14480 (2017).
[20] C. Paulsen, D. J. Hykel, K. Hasselbach, and D. Aoki, Phys. Rev. Lett. **109**, 237001 (2012).
[21] See Supplemental Material at http://link.aps.org/supplemental/10.1103/PhysRevB.103.L180501 for (1) details on the single-crystal growth, (2) the determination of the thermodynamic critical field, (3) additional hysteresis very close to T_c, (4) different methods to determine the lower critical field H_{c1}, and discussions on the anisotropy of H_{c1}, which includes Refs. [34–37].
[22] S. Sundar, S. Gheidi, K. Akintola, A. M. Côté, S. R. Dunsiger, S. Ran, N. P. Butch, S. R. Saha, J. Paglione, and J. E. Sonier, Phys. Rev. B **100**, 140502(R) (2019).
[23] F. Gömöry, Supercond. Sci. Technol. **10**, 523 (1997).
[24] C. P. Bean, Rev. Mod. Phys. **36**, 31 (1964).
[25] M. Naito, A. Matsuda, K. Kitazawa, S. Kambe, I. Tanaka, and H. Kojima, Phys. Rev. B **41**, 4823 (1990).
[26] E. Morosan, L. Li, N. P. Ong, and R. J. Cava, Phys. Rev. B **75**, 104505 (2007).
[27] L. Jiao, S. Howard, S. Ran, Z. Wang, J. O. Rodriguez, M. Sigrist, Z. Wang, N. P. Butch, and V. Madhavan, Nature **579**, 523 (2020).
[28] V. G. Kogan, R. Prozorov, and A. E. Koshelev, Phys. Rev. B **100**, 014518 (2019).
[29] V. G. Kogan, Phys. Rev. B **66**, 020509(R) (2002).
[30] J. D. Fletcher, A. Carrington, O. J. Taylor, S. M. Kazakov, and J. Karpinski, Phys. Rev. Lett. **95**, 097005 (2005).
[31] S. M. Thomas, F. B. Santos, M. H. Christensen, T. Asaba, F. Ronning, J. D. Thompson, E. D. Bauer, R. M. Fernandes, G. Fabbris, and P. F. S. Rosa, Sci. Adv. **6**, eabc8709 (2020).
[32] I. M. Hayes, D. S. Wei, T. Metz, J. Zhang, Y. S. Eo, S. Ran, S. R. Saha, J. Collini, N. P. Butch, D. F. Agterberg, A. Kapitulnik, and J. Paglione, arXiv:2002.02539.
[33] S. Kittaka, Y. Shimizu, T. Sakakibara, A. Nakamura, D. Li, Y. Homma, F. Honda, D. Aoki, and K. Machida, Phys. Rev. Research **2**, 032014(R) (2020).
[34] D. Aoki, T. D. Matsuda, F. Hardy, C. Meingast, V. Taufour, E. Hassinger, I. Sheikin, C. Paulsen, G. Knebel, H. Kotegawa, and J. Flouquet, J. Phys. Soc. Jpn. **80**, SA008 (2011).
[35] K. Deguchi, E. Osaki, S. Ban, N. Tamura, Y. Simura, T. Sakakibara, I. Satoh, and N. K. Sato, J. Phys. Soc. Jpn. **79**, 083708 (2010).
[36] S. Imajo, Y. Kohama, A. Miyake, C. Dong, M. Tokunaga, J. Flouquet, K. Kindo, and D. Aoki, J. Phys. Soc. Jpn. **88**, 083705 (2019).
[37] G. Knebel, M. Kimata, M. Vališka, F. Honda, D. Li, D. Braithwaite, G. Lapertot, W. Knafo, A. Pourret, Y. J. Sato, Y. Shimizu, T. Kihara, J.-p. Brison, J. Flouquet, and D. Aoki, J. Phys. Soc. Jpn. **89**, 053707 (2020).